Environ. Sci. Technol. **1999**, *33,* 546−552

Conformational Modeling of a New Building Block of Humic Acid: Approaches to the Lowest Energy Conformer

LAWRENCE T. SEIN, JR.,[†] JAMES M. VARNUM,[‡] AND SUSAN A. JANSEN*,[†]

Department of Chemistry, Temple University, Philadelphia, Pennsylvania 19122, and Kimmel Cancer Center, Thomas Jefferson University, Philadelphia, Pennsylvania 19107

Multiple structural models of humic acid (HA) building blocks have been reported. In this work, the modeling is based on two structural motifs: (i) the Steelink structure and (ii) a new humic acid [TNB] building block, which incorporates more fully the results of experimental data and retro-biosynthetic analyses. Both have significant conformational freedom complicated by their stereochemistry. A molecular modeling approach for the analysis of complex molecules with significant conformational freedom is described as it relates to the newly proposed humic acid building block. A potential energy surface for various conformers of the low-energy stereoisomer has been generated. Included in this discussion is the relationship of the stereochemistry to conformation and secondary structure.

Introduction

Although humic acid (HA) has been studied extensively for its remarkable environmental, biochemical, and therapeutic properties (*1*−*22*), little extensive modeling on HA has been performed, due in part to the incredible structural diversity in each of the proposed building block (BB) structures (*23, 24*). Until recently, the primary structure of the BB was poorly defined. The most commonly accepted models show the potential for multiple conformational isomers. Some appear so random that they cannot be easily linked to common biological raw materials (*23, 25*). Since humic-like materials are found in living plants (*2, 3, 26*−*28*), it is anticipated that their structure(s) will be well-defined, having resulted from controlled biosynthesis from a limited number of components (*29*) or from abiotic reactions involving biological degradation products. Our HA models possess multiple chiral centers. The first is the Steelink model, and the second is the TNB (Temple−Northeastern−Birmingham) structure as described previously (*27, 29*) (Figure 1).

Molecular modeling of such complex structures as these proposed HA BBs (Figure 1) presents unique problems (*30*). The standard approach is to minimize the energy of a trial geometry. The molecule is then subjected to molecular dynamics (MD) or simulated annealing (*31, 32*) to search conformational space. Resulting conformations are minimized in search of a global minimum. For complex systems, this cycle must be repeated using different starting geometries. This is an inefficient way to search conformational space, especially for complicated structures such as those in Figure 1 (*33*). Searching methods have been developed to address these problems (*30, 32, 34*−*37*). Deterministic methods systematically alter torsion angles (*33*), theoretically allowing a complete search of conformational space (*33, 34*). Stochastic methods (*30, 32, 35*−*39*) (Monte Carlo searches; *40, 41*) generate geometries using (pseudo)random variations in molecular geometry. Stochastic methods can vary internal coordinates, interatomic distances, or torsion angles. Random searching methods allow inversion of chiral centers, which is important when the stereochemical configuration is unknown.

Another peculiarity of conformer searching of HA BBs is that, in contrast to proteins, polypeptides (*42, 43*), and

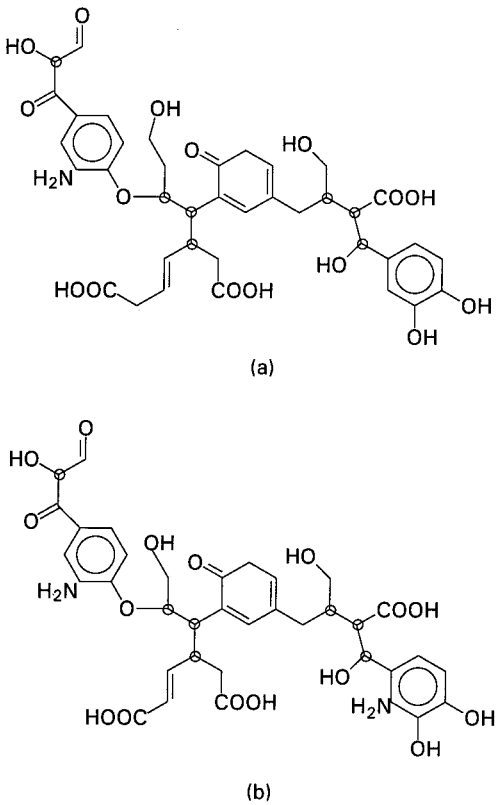

FIGURE 1. Molecular structure of (a) Steelink and (b) TNB humic acid monomers showing chiral centers as open circles.

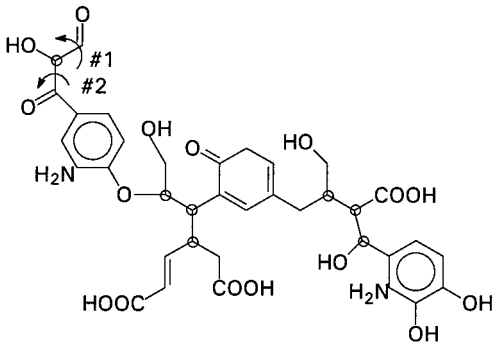

FIGURE 2. Molecular structure of TNB HA monomer showing bond torsions varied. See text for details.

* Corresponding author phone: (215)204-7118, ext 1470; fax: (215)204-1532.
[†] Temple University.
[‡] Thomas Jefferson University.

10.1021/es9805324 CCC: $18.00
Published on Web 12/18/1998

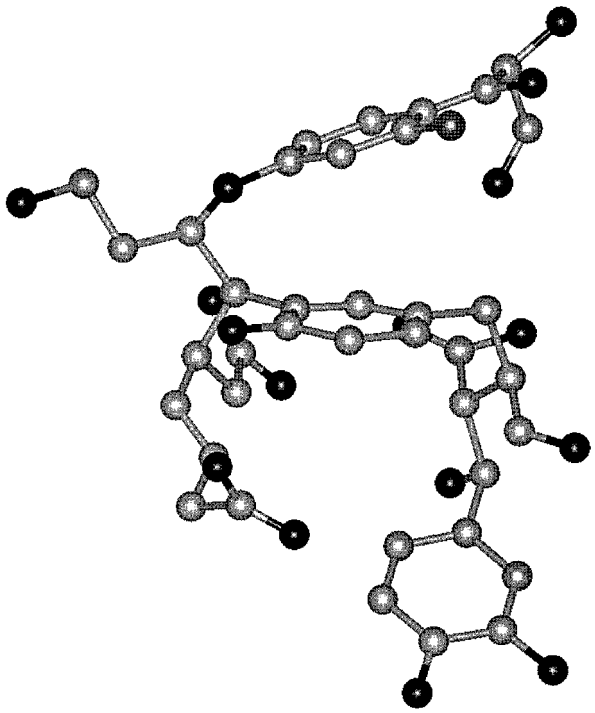

FIGURE 3. Lowest energy Steelink HA monomer as determined by RIPS search. Carbon atoms are light gray, nitrogen atoms are dark gray, oxygen atoms are black. Hydrogen atoms are not shown for clarity.

polysaccharides (*44*), the absolute and relative chiral configuration of HA monomer is unknown. This elevates the conformational problem to a level of complexity not normally encountered in conventional biomolecules. This necessitates a conformational searching algorithm that allows chiral inversion (*45*).

Molecular Modeling Methods

The modeling of biological materials requires conformational sampling. Low-energy geometries are obtained from multiple searching methods and dynamics minimizations. In most cases, the absolute stereochemical configuration is known, and the greatest difficulty is the modeling of the higher order structural features. In this work, the basic units have only ninety-some atoms, but each is stereochemically complex, having seven chiral centers.

The basic HA building block structure was produced using the Sketch utility of Sybyl (Tripos). For the Steelink model, all 64 chemically unique stereoisomers of HA were produced. All were optimized using the Tripos force field (*46*) and the Fletcher−Powell (*47*) conjugate−gradient minimization algorithm. The five lowest energy stereoisomers were then used as the starting geometries for random conformational searching using Sybyl. New conformers were obtained by randomly varying coordinates; retaining the structure if the energy was reasonable, optimizing the structure, and then repeating until "duplicate" structures were found. This approach allows for sampling the conformational space of many stereoisomers. The lowest energy structures from the random searches were further examined by molecular dynamics (*34*). The method used is based on the RIPS

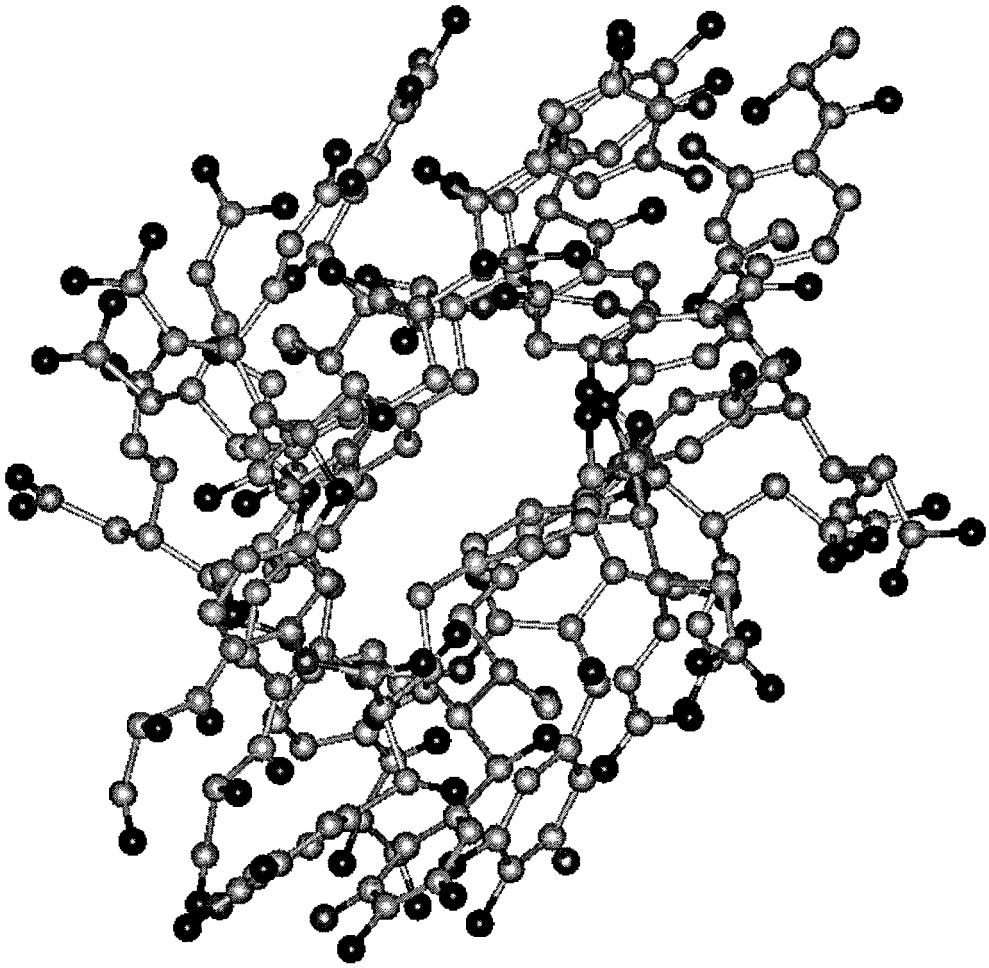

FIGURE 4. Hexamer of amide-linked HA BBs with view along helical axis. Color code as in Figure 3.

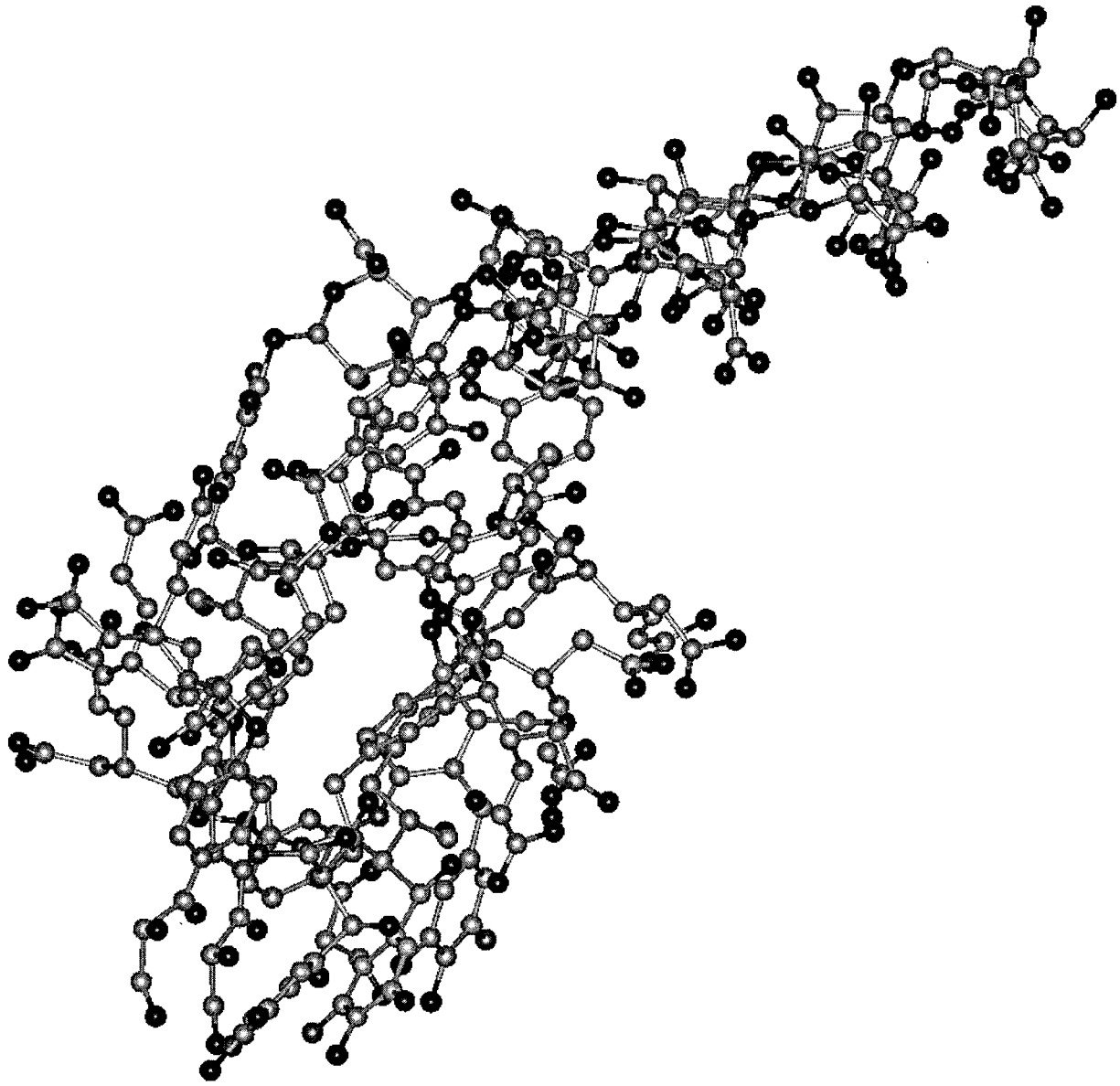

FIGURE 5. Hexamer of HA showing pendant polysaccharide. Actual saccharide depicted is alginic acid [poly(L-mucoronic, D-glucoronic acid)]. Color code as in Figure 3.

TABLE 1. Single-Point Energies of Lowest Energy HA Stereoisomers

	Steelink[a]	TNB[a]
RRRSRSS	−9906.90	−9783.33
RRRSSRS	−9914.08	−9785.28
SRRRRSS	−9895.23	−9790.97
SRRRSRS	−9902.82	−9793.22
SRRSRRS	−9923.20	−9785.73
SRRSRSR	−9916.41	−9780.54
SRRSSRR	−9907.71	−9787.77

[a] Energies in kcal/mol, as determined by PM3.

TABLE 2. Folding of Selected HA Stereoisomers

	Steelink[a]	TNB[a]
RRRSRSS	6.25	6.16
RRRSSRS	6.43	5.66
SRRRRSS	5.92	6.38
SRRRSRS	6.23	6.38
SRRSRRS	5.95	5.77
SRRSRSR	6.12	6.23
SRRSSRR	6.62	6.75

[a] Radius of gyration in Å (*51*).

algorithm of Houk et al. (*34*); it is a proprietary component of Sybyl (*46*).

The TNB model was assessed in similar manner. Because of the analogy of the TNB and Steelink models, the initial starting geometries for the TNB structures were obtained from modifications to the fully minimized Steelink structures. Molecular dynamics simulations used a constant-temperature bath of 300 and 400 K for 20 ps with both TRIPOS (*46*) and MM+ (*48*) force fields. Solvation studies used a periodic box of 1738 water molecules.

All structures were subjected to a simulated annealing protocol using the standard ensemble. Molecules were slowly "heated" from 300 to 600K and back to 300 K over 10 ps.

Quantum Mechanical Methods. PM3 (*49*) semiempirical calculations were performed on the both Steelink and TNB HA models (Table 1) to determine the single-point energies, using the HyperChem suite of programs (*50*). The RSSRSSR

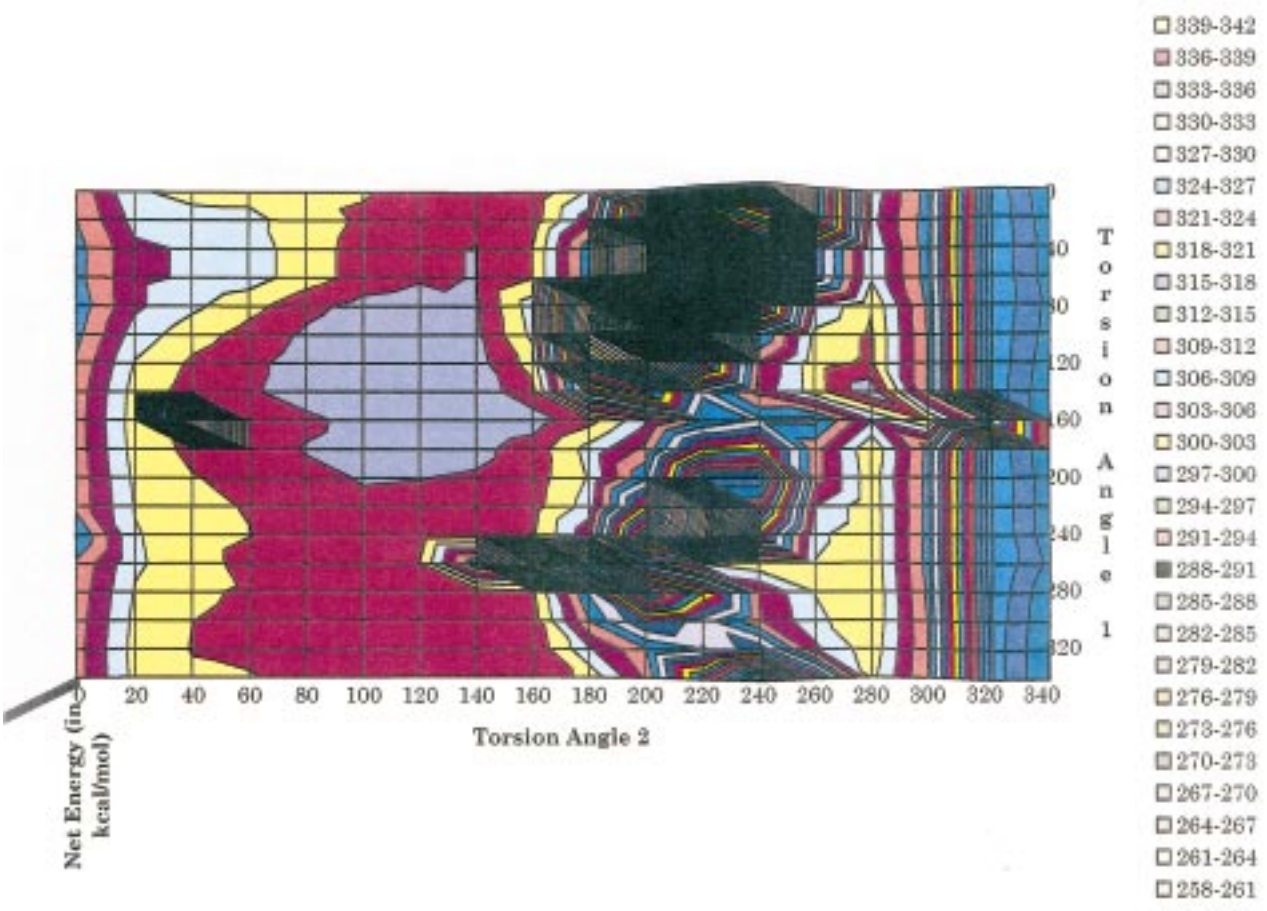

FIGURE 6. Net energy of TNB HA monomer from simultaneous rotation about two bonds (in kcal/mol) by PM3. See Figure 2 for bond definition.

(═SRRSRSS) conformer is consistently the lowest in energy. The radius of gyration (*51*) (Table 2) for each of the monomers was also calculated to demonstrate that there is no simple connection between the gross degree of monomer folding and the energy. Testing of conformational stability was achieved by varying two critical torsion angles for the TNB model (isomer RSSRSSR) as indicated in Figure 2.

Results and Discussion

The proposed HA BB model (Figure 1) is based on the average structural unit of HA obtained from chemical analysis (*1, 22, 27, 29, 52*). The TNB structure is consistent with several of those reported previously (*52, 53*). It is proposed to be the universal average formula unit of HA. The prevalence of C-6+3 units is a consequence of the phenylpropane degradation products in the work of Steelink (*52*). Other model structures contain monomers so large and so complex that the probability of their being either biosynthesized or spontaneously self-assembled on inorganic templates seems questionable (*23, 25*). These large structures contain Steelink- and TNB-like domains, suggesting a smaller, more well-defined subunit. Though Py-MS data has been interpreted as implying numerous HA monomers, these interpretations are open to question as changes of even 0.01 atm in the ion source pressure in CI systems can produce additional ions in biopolymers (*54, 55*). Even Py-GC/MS is only effective for polymers that can undergo "thermal scissions of macro-chain bonds" (*56, 57*); the influence of the extensive metal, sugar, and amino acid cross-linking (*25, 27−29, 53, 58, 59*) found ubiquitously in soil-derived HA on the interpretation of Py-MS data remains to be clarified. C-13 data is not conclusive either since (i) the failure to remove polysaccharide and amino acid contaminants skews the resulting spectra (*25, 27−29, 53*) and (ii) the presence of metals (*27−29, 58, 59*) may cause differential relaxation of various carbon atoms in the sample.

Our modeling studies have determined the relative energies for all the stereoisomers of the parent BB structure. Five independent random structural searches were performed to determine if the low-energy structure could be attributed to a particular stereoisomer. These searches produced >2000 unique structures each. The stereoisomer RSSRSSR was consistently produced as the lowest energy conformation, even when different starting stereoisomers were used. The same general conformation of RSSRSSR also was observed, and the gross features of these structures are similar. The lowest energy RSSRSSR structure was always 2−4 kcal/mol more stable than the next lowest energy species. All RSSRSSR conformations (Figure 3) show two important features. The first is a region I in which aromatic rings "stack" provide a large van der Waals stabilization. The second region 55 shows an alignment of two carboxylate groups. Both sites may be important for metal binding (*27, 58, 59*).

The low-energy structure RSSRSSR was then subjected to a constant temperature in vacuo molecular dynamics simulation. No significant changes in the structure were observed during the simulation. Solvation of the Steelink structure was assessed for both charged and uncharged species, since it would anticipated that carboxylate groups would be predominately deprotonated near neutral pH (*60*). There was a slight rotation of H-bonding function groups toward the nearby water molecules. The gross overall folding remained largely unaffected, and there was no reordering of the isomers in terms of energy.

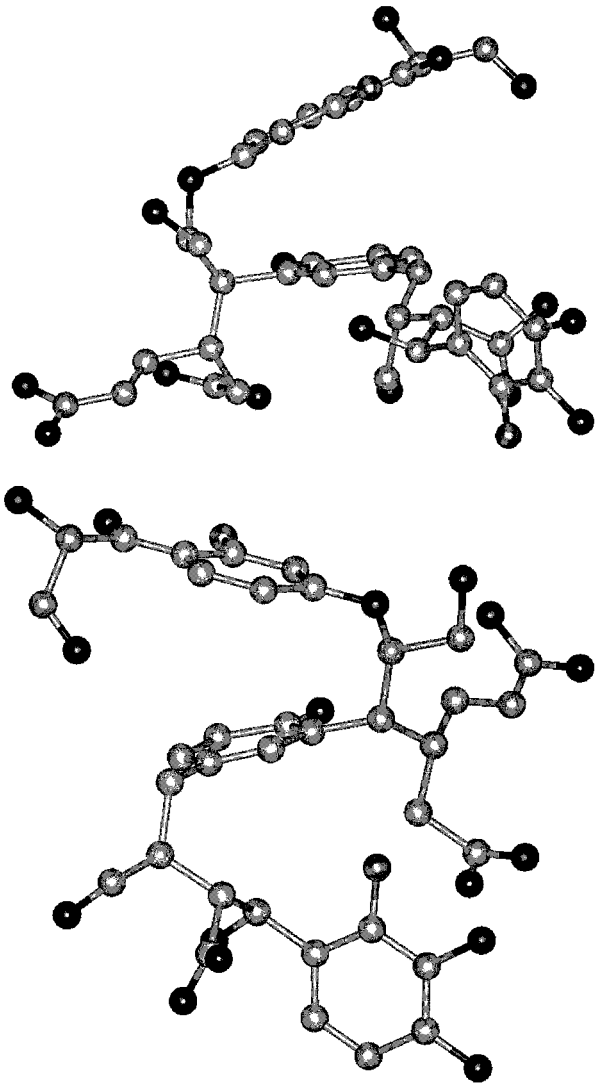

FIGURE 7. Molecular structure of high- and low-energy TNB HA conformers as determined by RIPS search. Color code as in Figure 3.

The low-energy TNB structures were obtained similarly. Because of the close structural similarity, the 10 lowest energy stereoisomers from the Steelink-64 were used as templates for the TNB minimization. These structures were then subjected to molecular dynamics protocols. The general conformational features and relative energies of stereoisomers were largely unaffected by dynamics minimization.

The conformational stability has also been assessed by semiempirical quantum methods. Since the molecular modeling of HA yielded showed a single low-energy stereoisomer with significant conformational stability, semiempirical quantum mechanical methods were applied to generate a potential energy surface for specific torsions (Figure 2). By varying the two torsion angles indicated simultaneously, a potential energy surface can be developed (Figure 6). This figure provides some interesting insight into the modeling problem. Normal torsional or dynamics minimization does not consistently give a low-energy structure like the "folded" structure observed for HA. This is because chiral inversions are not allowed, and therefore the folding cannot occur. For significant domains of the conformational space, the potential energy curve(s) are flat with only small energy differences observed within the domains. Other regions show sharp high-energy features where standard algorithms are likely to fail. Destabilizing factors are predominately subtle electronic factors, as the high-energy conformer has its two carbonyls and one hydroxyl group out of plane, thereby preventing stabilization by delocalization of π electrons or keto−enol isomerization.

Table 1 compares the energy of the low-energy Steelink structures to those of TNB. Stereochemical assignments for the TNB and Steelink models are consistent with a biosynthesis from tyrosine, phenylalanine, or tryptophan (*29*). The fundamental differences between the Steelink and TNB models relate to basic chemical considerations (Figure 1).

Chemical studies suggest that the amide linkage is critical to oligomerization of HA BB. A series of BB oligomers were examined. Preliminary studies show that a link between the amine and carboxylate of these molecules generates a stable helical structure (Figures 4 and 5) under MD simulation. Only the RSSRSSR isomer forms a helix; the others result in random coils. The helical nature of HA generates a coil with an 8.9 Å repeat distance (pitch) and an exterior surface containing potentially charged functional groups—carboxylate, phenolic and amine—on alternate faces. Because of the helical nature of the propagation, the occurrence of these groups is periodic.

Figure 8 shows a map of the functional groups at the HA surface as a function of translation distance. The translational distance is the arc length *s* of the elliptical helical curve. These functional groups may be binding sites for highly charged metallic species such as Cu^{2+} and Fe^{3+}, which are anticipated to cross-link HA chains (*27, 58, 59*). Higher order

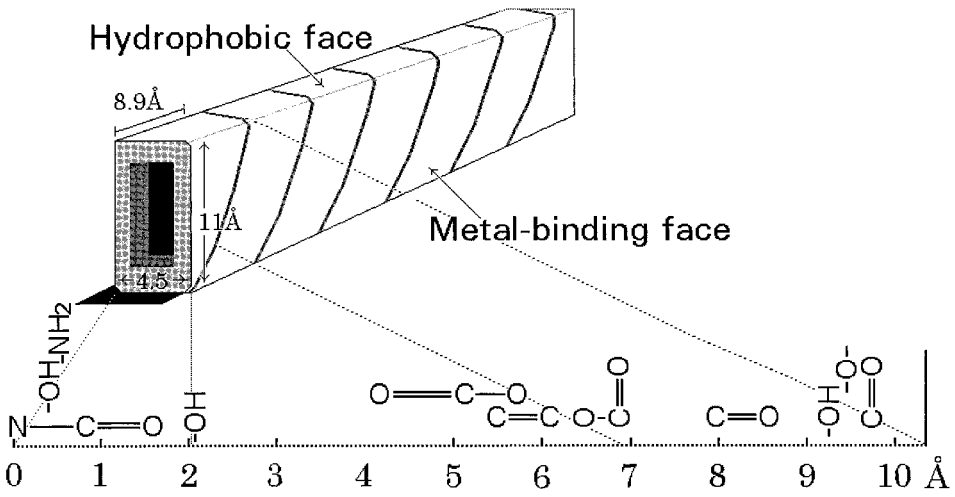

FIGURE 8. Schematic diagram of the distribution of functional groups around HA helix.

HA structure is therefore dependent on metal ion distribution (*59*).

The interior of the HA helix contains more hydrophobic functional groups, such as the carbonyl groups of ketones or aldehydes, that may be more selective in metal binding. From mercury loading and XANES and EXAFS studies (*27*), it has been proposed that the carbonyl groups form the ligand field for Hg in the HA. This view of a helical HA with a semi-hydrophilic surface and hydrophic interior mirrors the micelle model for HA aggregates proposed by Wershaw (*53*).

These modeling studies suggest that a single low-energy stereoisomer may exist for HA BBs. The relative configurations determined in this modeling work are identical to those anticipated from biosynthesis (*29*). This HA model hints at propagation mechanisms and metal binding functions of HA important for plant biochemistry and biomineralization

This extensive conformational analysis of a humic acid building block yielded a single low-energy isomer, RSSRSSR, significantly stabilized by van der Waals interaction between two stacked rings (Figure 3). The RSSRSSR isomer is consistent with the proposed biosynthesis of HA and other lignin-like species. Both the primary and secondary structures have implications for metal binding. The sterically unhindered location of the amine and one of the carboxylic acid groups indicates that these may be important in humic acid growth. Spectroscopic evidence supports the presence of an amide linkage. Other functional groups are available for metal ion exchange.

The combined use of random conformational searching and traditional modeling methods allows for a more complete analysis of HA conformation. The method described here should be applicable in general to systems possessing structural and stereochemical complexity.

Literature Cited

(1) Ziechmann, W. *Humic Substances*; BI Wissenschaftsverlag: Mannheim, 1993.
(2) Ghabbour, E. A.; Khairy, A. H.; Cheney, D. P.; Gross, V.; Davies, G.; Gilbert, T. R.; Zhang, X. *J. Appl. Phycol.* **1994**, *6*, 459.
(3) Radwan, A.; Davies, G.; Fataftah, A.; Ghabbour, E. A.; Jansen, S. A.; Willey, R. J. *J. Appl. Phycol.* **1997**, *8*, 553.
(4) Davies, G.; Ghabbour, E. A.; Khairy, A. H.; Ibrahim, H. Z. *J. Phys. Chem. B* **1997**, *101*, 3328.
(5) Senesi, N., Miano, T. M., Eds. *Humic Substances in the Global Environment: Implications for Human Health*; Elsever, Amsterdam, 1994.
(6) (a) Khairy, A. H. *Acta Med. Empirica* **1981**, *11*, 898. (b) Khairy, A. H. *De Natura Rerum* **1989**, *3*, 229. (c) Khairy, A. H.; El-Gendi, S. S.; Bhagdadi, H. H. *De Natura Rerum* **1991**, *5*, 76. (d) Klockling, R.; Eichhorn, U.; Blumohr, T. *Fresenius Z. Anal. Chem.* **1978**, *292*, 408.
(7) Golbs, S.; Volkhard, F.; Kuchnert, M. *Arch. Exp. Veternaermed.* **1982**, *36*, 179.
(8) Seubert, B.; Belharz, H.; Fickert, W.; Jeromin, G.; Spitaler, U. U.S. Patent 4,918,059, 1990.
(9) Lin, J.-K.; Lee, S.-F. *Mutat. Res.* **1992**, *229*, 217.
(10) Golbs, S.; Kuchnert, M.; Fuchs, V. *Z. Ges. Hyg.* **1984**, *30*, 720.
(11) Golbs, S.; Volkhard, F.; Kuchnert, M. *Arch. Exp. Veternaermed.* **1982**, *36*, 179.
(12) Klöcking, R.; Eichhorn, U.; Blumohr, T. *Fresenius Z. Anal. Chem.* **1978**, *292*, 408.
(13) Khairy, A. H.; Ibrahim, H. Z.; Ghabbour, E.; Davies, G. *J. Phys. Chem.* **1996**, *100*, 2410.
(14) Khairy, A. H.; Ibrahim, H. Z.; Ghabbour, E.; Davies, G. *J. Phys. Chem.* **1996**, *100*, 7.
(15) (a) Khairy, A. H.; Baghdadi, H. H.; Ghabbour, E. A. *Z. Pflanzenernahr. Bodenkd.* **1990**, *153*, 33. (b) Flaig, W. *Sci. Proc. R. Dublin Soc.* **1960**, *4*, 49.
(16) Golbs, S.; Kuchnert, M.; Fuchs, V. *Z. Ges. Hyg.* **1984**, *30*, 720.
(17) Tao, Z.; Du, J. *Radiochim. Acta* **1994**, *64*, 225.
(18) Hall, G.; MacLaurin, A.; Vaive, J. *J. Geochem. Explor.* **1995**, *54*, 27.
(19) (a) Sato, T.; Ose, Y.; Nagase, H. *Mutat. Res.* **1986**, *162*, 173. (b) Sato, T.; Ose, Y.; Nagase, H.; Hayase, K. *Sci. Total Environ.* **1987**, *62*, 305.
(20) (a) Gulyas, H.; von Bismarck, R.; Hemmerling, L. *Water. Sci. Technol.* **1995**, *32*, 127. (b) Fuchs, W. *Kolloid Z.* **1930**, *52*, 124. (c) See also *Surface and Colloid Chemistry in Natural Water and Water Treatment*; Beckett, R., Ed.; Plenum: New York, 1990; pp 3−20.
(21) Ghio, A. J.; Quigley, D. R. *Am. Physiol. Soc.* **1994**, *267*, L382.
(22) Ghio, A. J.; Quigley, D. R. *Am. Physiol. Soc.* **1994**, *266*, L173.
(23) Schnitzer, M. Humic substances: Chemistry and reactions. In *Soil Organic Matter*; Schnitzer, M., Khan, S. U., Eds.; Elsevier: New York, 1978; pp 1−58.
(24) *Humic Substances II: In Search of Structures*; Hayes, M. H. B., MacCarthy, P., Malcolm, R. L., Swift, R. S., Eds.; Wiley: New York, 1989.
(25) Schnitzer, H.-R.; Schulten, M. *Naturwissenschaften* **1995**, *82*, 487.
(26) Ghabbour, E. A.; Khairy, A. H.; Cheney, D. P.; Gross, V.; Davies, G.; Gilbert, T. R.; Zhang, X. *J. Appl. Phycol.* **1994**, *6*, 459.
(27) Davies, G.; Fataftah, A.; Cherkassiy, A.; Ghabbour, E. A.; Radwan, A.; Jansen, S. A.; Kolla, S.; Paciolla, M. D.; Sein, L. T., Jr.; Buermann, W.; Balasubramanian, M.; Budnick, J.; Xing, B. *J. Chem. Soc., Dalton Trans.* **1997**, 4047.
(28) Jansen, S. A.; Kolla, S.; Sein, L. T., Jr.; Varnum, J. M.; Paciolla, M. D.; Radwan, A.; Ghabbour, E. A.; Davies, G. Distribution of polysaccharides in humic acid derived from plant sources. In *The Role of Humic Substances in the Ecosystems and in Environmental Protection*; Drozd, J., Gonet, S. S., Senesi, N., Weber, J., Eds.; Polish Society of Humic Substances: Wroclaw, Poland, 1997; p 157.
(29) Kolla, S.; Sein, L. T., Jr.; Paciolla, M. D.; Jansen, S. A. *Recent Res. Adv. Phys. Chem.* **1998**, *2*, 22.
(30) Beutler, T. C.; Dill, K. A. *Protein Sci.* **1996**, *5* (10), 2037.
(31) Annealing is the technique used for recrystallization, in which the molecule is cooled very slowly, so as not to lock in regions of disorder. Simulated annealing is a computational technique to mimic this process. See: (a) Metropolis, M. A.; Rosenbluth, A.; Rosenbluth, M.; Teller, A.; Teller, E. *J. Chem. Phys.* **1953**, *21* (6), 1087. (b) Kirkpatrick, S.; Gelatt. C. D., Jr.; Vecchi, M. P. *Science* **1983**, *220*, 4598.
(32) Jones, G.; Wilett, P.; Glen, R. C. *Proc. Int. Chem. Inf. Conf.* **1994**, 135.
(33) Ferguson, D. M.; Raber, D. J. *J. Am. Chem. Soc.* **1989**, *111*, 4371.
(34) Saunders, M.; Houk, K. N.; Wu, Y.; Still, C.; Lipton, M.; Chang, G.; Guida, W. C. *J. Am. Chem. Soc.* **1990**, *111*, 1419−1427.
(35) Taylor, N. R.; von Itzstein, M. *J. Comput.-Aided Mol. Des.* **1996**, *10* (3), 233.
(36) Treasurywala, A. M.; Jaeger, E. P.; Peterson, M. L. *J. Comput. Chem.* **1996**, *17* (9), 1171.
(37) Hao, M.-H.; Scheraga, H. A. *J. Phys. Chem.* **1994**, *98*, 9882.
(38) Knack, I.; Roehm, K. H. *Z. Naturforsch C: Biosci.* **1981**, *36* (3−4), 347.
(39) Baysal, C.; Meirovitch, H. *J. Phys. Chem. A* **1997**, *101* (11), 2185.
(40) Li, Z.; Scheraga, H. A. *Proc. Natl. Acad. Sci. U.S.A.* **1987**, *84*, 6611.
(41) Vasquez, M.; Meirovitch, E.; Meirovitch, H. *J. Phys. Chem.* **1994**, *98*, 9380.
(42) Gouda, H.; Matsuzaki, K.; Tanaka, H.; Hirono, S.; Omura, S.; McCauley, J. A.; Sprengeler, P. A.; Furst, G. T.; Smith, Amos, B., III. *J. Am. Chem. Soc.* **1996**, *118*, 13087.
(43) Kolossvary, I.; Guida, W. C. *J. Am. Chem. Soc.* **1996**, *118*, 5011.
(44) Midland, M. M.; Asirwatham, G.; Cheng, J. C.; Miller, J. A.; Morell, L. *J. Org. Chem.* **1994**, *59*, 4438.
(45) Weinberg, N.; Wolfe, S. *J. Am. Chem. Soc.* **1994**, *116*, 9860.
(46) Modeling performed using Sybyl 6.1 on a single processor R/4000 Silicon Graphics workstation. Convergence was accelerated by use of Pulay's Direct Inversion of the Iterative Subspace (DIIS) method (*61*). Nonbonded interaction cutoff set to 8.0 Å. Maximum cycles = 1000; energy cutoff = 70 kcal/mol. RMS forces criterion = 0.2 kcal/(Å mol); convergence threshold = 0.005 kcal/mol. Option "Check chiral" set to NO to allow chiral inversion. Dielectric was set to constant; partial charges were calculated using bond dipoles. Tripos force field is designed to model large biomolecules; it is a proprietary product of Tripos, St. Louis, MO.
(47) Fletcher, R.; Powell, M. J. D. *J. Comput.* **1963**, *6*, 163.
(48) MM+ is an extension of the MM2 force field of Allinger et al. with additional parameters. MM+ was designed to model small organic molecules. See: (a) Allinger, N. L. *J. Am. Chem. Soc.* **1977**, *99*, 8127. (b) Allinger, N. L.; Yuh, Y. H. *Quantum Chemistry Program Exchange*; Bloomington, IN, Program 395, Molecular Mechanics; Burkert, U., Allinger, N. L., Eds.; ACS Monograph 177; American Chemical Society: Washington, DC, 1982. (c) Lii, J.; Gallion, S.; Bender, C.; Wikstrom, H.; Allinger, N. L.; Flurchick, K. M.; Teeter, M. M. *J. Comput. Chem.* **1989**, *10*, 503.

(d) Lipkowitz, K. B. *QCPE Bull.* **1992**, *12*, 1. Convergence was accelerated by use of Pulay's Direct Inversion of the Iterative Subspace (DIIS) method (*61*). Nonbonded interaction cutoff set to 8.0 Å. Maximum cycles = 1000; energy cutoff = 70 kcal/mol. RMS forces criterion = 0.2 kcal/(Å mol); convergence threshold = 0.005 kcal/mol. Option "Check chiral" set to NO to allow chiral inversion. Dielectric was set to constant; partial charges were calculated using bond dipoles.

(49) PM3 is a semiempirical quantum mechanical calculation method designed to remedy some of the deficiencies of AM1 when dealing with small organic molecules, especially those with heteroatoms. See: (a) Stewart, J. J. P. *J. Comput. Chem.* **1989**, *10*, 209. (b) Stewart. J. J. P. *J. Comput. Chem.* **1989**, *10*, 221. Convergence threshold was set to 0.1 kcal/mol. Accelerate convergence was OFF.

(50) HyperChem version 5.02. HyperChem is a trademark of Hypercube, Waterloo, Canada.

(51) Radius of gyration (R_g) is $(I/MW)^{1/2}$, where I is the moment of inertia of the molecule and MW is the molecular weight. I was determined from $I = (I_x^2 + I_y^2 + I_z^2)^{1/2}$ where I_x, I_y, and I_z are the principal moments of inertia as provided in the HyperChem Display Inertial Axes.

(52) Steelink, C. Implications of elemental characteristics of humic substances. In *Humic Substances in Soil, Sediments and water*; Aiken, G. R., McKnight, D. M., Wershaw, R. L., MacCarthy, P., Eds.; Wiley-Interscience: New York, 1985; pp 457−476.

(53) (a) Wershaw, R. L. *J. Contam. Hydrol.* **1986**, *1*, 29. (b) Wershaw, R. L. *Environ. Health Perfect.* **1989**, *83*, 191. (c) Wershaw, R. L. *U.S. Geol. Surv. Water-Supply Pap.* **1994**, *No. 2410*. (d) Wershaw, R. L. *Environ. Sci. Technol.* **1993**, *27*, 814. (e) Leenheer, J. A.; Wershaw, R. L.; Reddy, M. M. *Environ. Sci. Technol.* **1995**, *29*, 393.

(54) Snyder, A. P.; Liebman, S. A.; Schroeder, M. A.; Fifer, R. A. *Org. Mass Spectrosc.* **1990**.

(55) Snyder, A. P.; Eiceman, G. A.; Windig, W. *J. Anal. Pyrol.* **1988**, *13*, 243.

(56) Zaikin, V. G.; Filippova, V. G.; Semenov. *Org. Mass Spectrom.* **1991**.

(57) Schulten, H.-R.; Lattimer, R. P. *Mass Spectrom. Rev.* **1984**, *3*, 231.

(58) Jansen, S. A.; Varnum, J. M.; Kolla, S.; Paciolla, M. D.; Sein, L. T., Jr.; Nwabara, S.; Ghabbour, E. A.; Fataftah, A.; Davies, G. Metal uptake by metal-free humic acid. In *The Role of Humic Substances in the Ecosystems and in Environmental Protection*; Drozd, J., Gonet, S. S., Senesi, N., Weber, J., Eds.; Polish Society of Humic Substances: Wroclaw, Poland, 1997; p 741.

(59) Jansen, S. A.; Paciolla, M.; Chabbour, E. A.; Davies, G.; Varnum, J. M. *Mater. Sci. Eng.* **1996**, *C4*, 181.

(60) Note that other structural models, even when accounting for solvation, fail to account for the pK_a values of the relevant functional groups.

(61) (a) Pulay, P.; Fogarasi, G.; Pang, F.; Boggs, J. E. *J. Am. Chem. Soc.* **1979**, *101*, 2550. (b) Pulay, P.; Fogarasi, G. *J. Chem. Phys.* **1992**, *96*, 2856.

Received for review May 21, 1998. Revised manuscript received October 6, 1998. Accepted October 19, 1998.

ES9805324